J|A|C|S ARTICLES

Published on Web 09/30/2010

Structural Inhomogeneity of Interfacial Water at Lipid Monolayers Revealed by Surface-Specific Vibrational Pump−Probe Spectroscopy

Mischa Bonn,* Huib J. Bakker, Avishek Ghosh, Susumu Yamamoto, Maria Sovago, and R. Kramer Campen

FOM Institute AMOLF, Science Park 104, 1098 XG, Amsterdam, The Netherlands

Received July 13, 2010; E-mail: bonn@amolf.nl

Abstract: We report vibrational lifetime measurements of the OH stretch vibration of interfacial water in contact with lipid monolayers, using time-resolved vibrational sum frequency (VSF) spectroscopy. The dynamics of water in contact with four different lipids are reported and are characterized by vibrational relaxation rates measured at 3200, 3300, 3400, and 3500 cm^{-1}. We observe that the water molecules with an OH frequency ranging from 3300 to 3500 cm^{-1} all show vibrational relaxation with a time constant of $T_1 = 180 \pm 35$ fs, similar to what is found for bulk water. Water molecules with OH groups near 3200 cm^{-1} show distinctly faster relaxation dynamics, with $T_1 < 80$ fs. We successfully model the data by describing the interfacial water containing two distinct subensembles in which spectral diffusion is, respectively, rapid (3300−3500 cm^{-1}) and absent (3200 cm^{-1}). We discuss the potential biological implications of the presence of the strongly hydrogen-bonded, rapidly relaxing water molecules at 3200 cm^{-1} that are decoupled from the bulk water system.

1. Introduction

Biological membranes define the external boundaries of cells and organelles and are composed primarily of amphiphilic (phospho-)lipid molecules that spontaneously form bilayers. Membranes regulate the traffic of molecules into and out of cells. This functionality is principally realized by anchored or transmembrane proteins, whose structure/function relationship is the result of a delicate interplay of the proteins themselves, lipids, and interfacial water. For example, several recent studies have made clear that the proper functioning of various voltage-sensing transmembrane proteins requires both membrane-bound water and association with particular lipids.[1−4] Using model systems, others have shown that, even in the absence of protein, lipid hydration plays a critical role in both bilayer assembly and phase behavior.[5] While lipid/water interactions thus control many of the basic biophysical features of membranes, the resulting structures also lead to water properties that differ drastically from those of the bulk: for example, a number of NMR studies have shown that the mobility of membrane-bound water is 100 times slower than the mobility of water in the neat liquid.[6−8] Similarly, dielectric relaxation studies have demonstrated that the reorientational dynamics of membrane-bound water are greatly slowed.[9,10]

To quantitatively understand the thermodynamics of membrane assembly, transmembrane protein function, and the behavior of protons at the cell surface, we thus require insight into the local environment of water molecules at the membrane/water interface.[11−13] In principle, the OH stretch vibration of water could serve as a good reporter of the local water environment at the membrane interface: for strongly hydrogen-bonded water molecules, the OH stretch vibration is shifted to lower frequencies than for water hydrogen-bonded more weakly. The amount of this shift thus provides insight into the water local molecular environment.[14] To probe specifically the interfacial water molecules, we employ surface-specific, laser-based vibrational sum frequency (VSF) generation spectroscopy. VSF spectroscopy is a second-order nonlinear optical technique in which a visible and an infrared field are overlapped at an interface and the resulting emission at the sum of their frequencies is measured. This emission is generally restricted

(1) Freites, J.; Tobias, D.; von Heijne, G.; White, S. *Proc. Natl. Acad. Sci. U.S.A.* **2005**, *102* (42), 15059–15064.
(2) Schmidt, D.; Jiang, Q.-X.; Mackinnon, R. *Nature* **2006**, *444* (7120), 775–779.
(3) Krepkiy, D.; Mihailescu, M.; Freites, J. A.; Schow, E. V.; Worcester, D. L.; Gawrisch, K.; Tobias, D. J.; White, S. H.; Swartz, K. J. *Nature* **2009**, *462* (7272), 473–479.
(4) Johansson, A. C. V.; Lindahl, E. *J. Phys. Chem. B* **2009**, *113* (1), 245–253.
(5) Milhaud, J. *Biochim. Biophys. Acta: Biomembr.* **2004**, *1663* (1−2), 19–51.
(6) Zhou, Z.; Sayer, B.; Hughes, D.; Stark, R.; Epand, R. *Biophys. J.* **1999**, *76* (1), 387–399.
(7) Kurze, V.; Steinbauer, B.; Huber, T.; Beyer, K. *Biophys. J.* **2000**, *78* (5), 2441–2451.
(8) Gawrisch, K.; Gaede, H. C.; Mihailescu, M.; White, S. H. *Eur. Biophys. J. Biophys. Lett.* **2007**, *36* (4−5), 281–291.
(9) Klosgen, B.; Reichle, C.; Kohlsmann, S.; Kramer, K. D. *Biophys. J.* **1996**, *71* (6), 3251–3260.
(10) Tielrooij, K. J.; Paparo, D.; Piatkowski, L.; Bakker, H. J.; Bonn, M. *Biophys. J.* **2009**, *97* (9), 2484–2492.
(11) Mulkidjanian, A. Y.; Heberle, J.; Cherepanov, D. A. *Biochim. Biophys. Acta: Bioenerg.* **2006**, *1757* (8), 913–930.
(12) Sanden, T.; Salomonsson, L.; Brzezinski, P.; Widengren, J. *Proc. Natl. Acad. Sci. U.S.A.* **2010**, *107* (9), 4129–4134.
(13) Yamashita, T.; Voth, G. A. *J. Phys. Chem. B* **2010**, *114* (1), 592–603.
(14) Steiner, T. *Angew. Chem., Int. Ed.* **2002**, *41* (1), 48–76.

 © 2010 American Chemical Society

to the 1→2 molecular layers closest to the interface[15−17] and increases strongly when the infrared frequency is resonant with a vibration of surface molecules. Hence, for water overlaid by lipid monolayers, VSF spectroscopy provides the vibrational spectra of only the lipid-bound water. A number of VSF experiments at the water/lipid (and more generally water/surfactant) interface have revealed important insights into water interfacial structure and orientation.[18−26] Unfortunately, the spectral response of the OH stretch of membrane-bound interfacial water is broad (extending from 3100 to 3500 cm^{-1}) and relatively featureless (see Figure 1). It has therefore proven challenging to extract structural information from these spectra: to distinguish the influence of homogeneous (fast structural evolution or excitation transfer) and inhomogenous (different quasi-static types of interfacial water) line broadening effects on the OH stretch spectral response.[27−29] This situation is analogous to linear infrared absorbance and spontaneous Raman scattering studies of bulk water, where spectral line shapes contain inseparable homogeneous and inhomogeneous effects that render the interpretation of the spectra in terms of water structure or dynamics virtually impossible.[30−33]

It has been shown in the past few decades that ultrafast time-resolved vibrational pump−probe spectroscopies can do much to resolve this ambiguity for bulk water systems. In these experiments, a subensemble of the various OH groups is selectively excited by use of an intense ("pump") pulse, frequency-matched to some portion of the OH stretch. By monitoring the dissipation of this perturbation as a function of time between pump and probe pulses, insight into the dynamics of the underlying hydrogen-bonded network can be gained and the response of different structural types of water can be independently addressed.[34−47] This type of pump−probe experiment has recently been extended to study specifically water molecules at interfaces, by use of an infrared pump followed by a VSF probe (a second infrared and simultaneous visible pulse).[48−56] By employing an infrared pump in this scheme whose bandwidth is less than the width of the OH vibration, the relaxation dynamics (T_1) of different portions of the OH vibrational spectrum can be followed. This allows for direct probing of potentially different quasi-static water structural types.

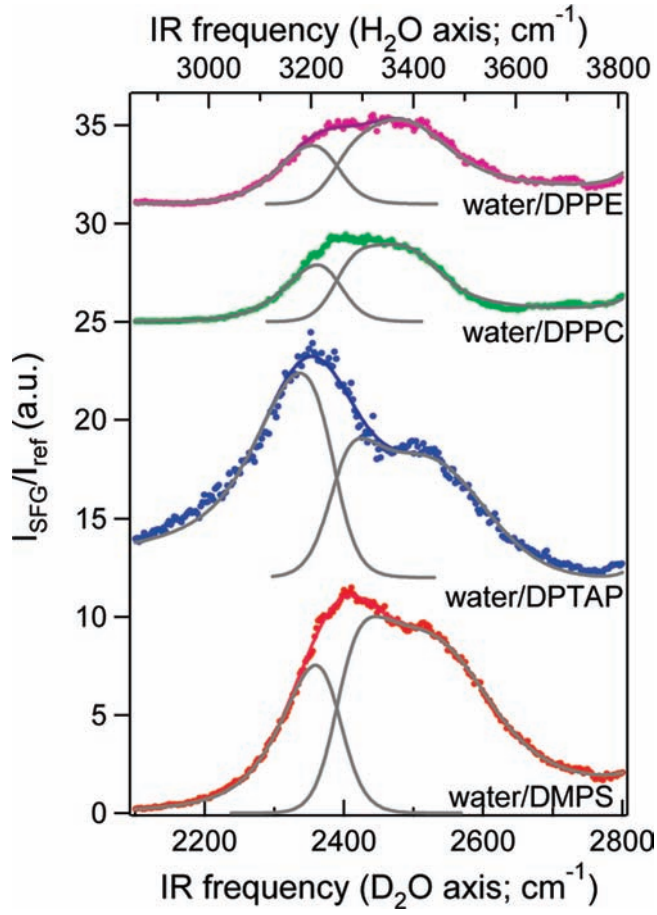

Figure 1. Static VSF spectra of D_2O at four different lipid interfaces. The vibrational response of H_2O at these interfaces is identical to that of D_2O, apart from a frequency scaling factor of 1.36. The corresponding H_2O frequency axis is shown on the top of the figure. Gray lines show the spectral decomposition separating the response at low and high frequencies, used in the simulation of the transients; for details, see the text. We note that the spectral decomposition should not be taken to imply "icelike" and "liquidlike" substructures.

(15) Shen, Y. R. *Nature* **1989**, *337* (6207), 519–525.
(16) Shen, Y. *Surf. Sci.* **1994**, *299* (1−3), 551–562.
(17) Shen, Y. *IEEE J. Sel. Top. Quantum Electron.* **2000**, *6* (6), 1375–1379.
(18) Gragson, D.; McCarty, B.; Richmond, G. *J. Phys. Chem.* **1996**, *100* (34), 14272–14275.
(19) Bell, G.; Bain, C.; Ward, R. *J. Chem. Soc., Faraday Trans.* **1996**, *92* (4), 515–523.
(20) Miranda, P.; Du, Q.; Shen, Y. *Chem. Phys. Lett.* **1998**, *286* (1−2), 1–8.
(21) Watry, M.; Tarbuck, T.; Richmond, G. *J. Phys. Chem. B* **2003**, *107* (2), 512–518.
(22) Viswanath, P.; Aroti, A.; Motschmann, H.; Leontidis, E. *J. Phys. Chem. B* **2009**, *113* (44), 14816–14823.
(23) Sovago, M.; Vartiainen, E.; Bonn, M. *J. Chem. Phys.* **2009**, *131* (16), 161107.
(24) Ma, G.; Liu, J.; Fu, L.; Yan, E. C. Y. *Appl. Spectrosc.* **2009**, *63* (5), 528–537.
(25) Wurpel, G. W. H.; Sovago, M.; Bonn, M. *J. Am. Chem. Soc.* **2007**, *129* (27), 8420–8421.
(26) Nagata, Y.; Mukamel, S. *J. Am. Chem. Soc.* **2010**, *132*, 1–9.
(27) Sovago, M.; Campen, R. K.; Bakker, H. J.; Bonn, M. *Chem. Phys. Lett.* **2009**, *470* (1−3), 7–12.
(28) Sovago, M.; Campen, R. K.; Wurpel, G. W. H.; Müller, M.; Bakker, H. J.; Bonn, M. *Phys. Rev. Lett.* **2008**, *101* (13), 139402.
(29) Sovago, M.; Campen, R. K.; Wurpel, G. W. H.; Müller, M.; Bakker, H. J.; Bonn, M. *Phys. Rev. Lett.* **2008**, *100* (17), 173901.
(30) Eaves, J.; Tokmakoff, A.; Geissler, P. *J. Phys. Chem. A* **2005**, *109* (42), 9424–9436.
(31) Geissler, P. *J. Am. Chem. Soc.* **2005**, *127* (42), 14930–14935.
(32) Auer, B. M.; Skinner, J. L. *J. Chem. Phys.* **2008**, *128* (22), 224511.
(33) Skinner, J. L.; Auer, B. M.; Lin, Y. *Adv. Chem. Phys.* **2009**, *142*, 59–103.
(34) Woutersen, S.; Emmerichs, U.; Bakker, H. J. *Science* **1997**, *278* (5338), 658–660.
(35) Woutersen, S.; Bakker, H. *Nature* **1999**, *402* (6761), 507–509.
(36) Laenen, R.; Simeonidis, K.; Laubereau, A. *J. Phys. Chem. B* **2002**, *106* (2), 408–417.
(37) Asbury, J.; Steinel, T.; Kwak, K.; Corcelli, S.; Lawrence, C.; Skinner, J.; Fayer, M. *J. Chem. Phys.* **2004**, *121* (24), 12431–12446.
(38) Nibbering, E.; Elsaesser, T. *Chem. Rev.* **2004**, *104* (4), 1887–1914.
(39) Fecko, C. J.; Loparo, J. J.; Roberts, S. T.; Tokmakoff, A. *J. Chem. Phys.* **2005**, *122* (5), 054506.
(40) Huse, N.; Ashihara, S.; Nibbering, E.; Elsaesser, T. *Chem. Phys. Lett.* **2005**, *404* (4−6), 389–393.
(41) Wang, Z.; Pakoulev, A.; Pang, Y.; Dlott, D. D. *J. Phys. Chem. A* **2004**, *108* (42), 9054–9063.
(42) Lindner, J.; Vohringer, P.; Pshenichnikov, M.; Cringus, D.; Wiersma, D.; Mostovoy, M. *Chem. Phys. Lett.* **2006**, *421* (4−6), 329–333.
(43) Ashihara, S.; Huse, N.; Espagne, A.; Nibbering, E.; Elsaesser, T. *Chem. Phys. Lett.* **2006**, *424* (1−3), 66–70.
(44) Ashihara, S.; Huse, N.; Espagne, A.; Nibbering, E. T. J.; Elsaesser, T. *J. Phys. Chem. A* **2007**, *111* (5), 743–746.
(45) Park, S.; Fayer, M. D. *Proc. Natl. Acad. Sci. U.S.A.* **2007**, *104* (43), 16731–16738.
(46) Bakker, H. J. *Chem. Rev.* **2008**, *108* (4), 1456–1473.
(47) Bakker, H. J.; Skinner, J. L. *Chem. Rev.* **2010**, *110* (3), 1498–1517.

Here we present an IR pump−VSF probe study of interfacial water beneath four different lipid monolayers, each with four different excitation/probing frequencies [where for each experiment the pump and probe frequencies are the same (one-color experiments)]. We have previously reported the results of similar one-color experiments for the neat air/water interface and 1,2-dimyristoyl-*sn*-glycero-3-[phospho-L-serine] (DMPS)/water interface.[49,52] At the air/water interface, we found that the water vibrational dynamics could be fully accounted for by the behavior previously reported for bulk water; time constants characterizing vibrational relaxation were both frequency-independent and had the same value as those for bulk water; the water OH stretch band was homogeneous in exactly the same sense as bulk H_2O.[34,35,57,58] Both McGuire and Shen[48] and Eftekari-Bafrooei and Borguet[55] have demonstrated similar behavior for the silica/water interface. In the former study at circumneutral pH, vibrational relaxation was found to be frequency-independent and quantitatively similar to bulk, while in the later study at pH 12, vibrational relaxation was shown to be frequency-independent and quantitatively similar to bulk, while at pH 2, frequency independence was preserved but relaxation was somewhat slowed. In contrast, for the DMPS/water interface we concluded that the spectral response was strongly inhomogeneous and characterized by different vibrational relaxation rates at 3200, 3300, 3400, and 3500 cm^{-1}, with faster relaxation occurring at lower vibrational frequencies, for which hydrogen bonding is stronger. In this study we extend that prior work by examining vibrational relaxation at three additional lipid monolayers and at the DMPS/water interface over longer time scales. This greatly enlarged data set, along with additional data analysis techniques, allows us to demonstrate that for all lipids this inhomogeneity is not complete over the OH stretch band but is instead partial: water molecules with an OH frequency ranging from 3300 to 3500 cm^{-1} show vibrational relaxation with similar time constants, while water molecules with OH groups near 3200 cm^{-1} show distinctly faster relaxation dynamics. There are a large number of experimental and computational studies of characteristics of water near membranes. Evaluated in this context, and given extensive prior studies of the vibrational relaxation of water in bulk, this population of fast-relaxing water at 3200 cm^{-1} can be most simply understood to be water near the base of the lipid hydrophilic headgroup. This conclusion can be tested by further, more complicated spectroscopic experiments. Water molecules located in this region of the lipid are thought to be important for a variety of biochemical processes—including but not limited to those discussed above—and thus we expect the ability to probe this specific water population to be of interest to a wide variety of workers.

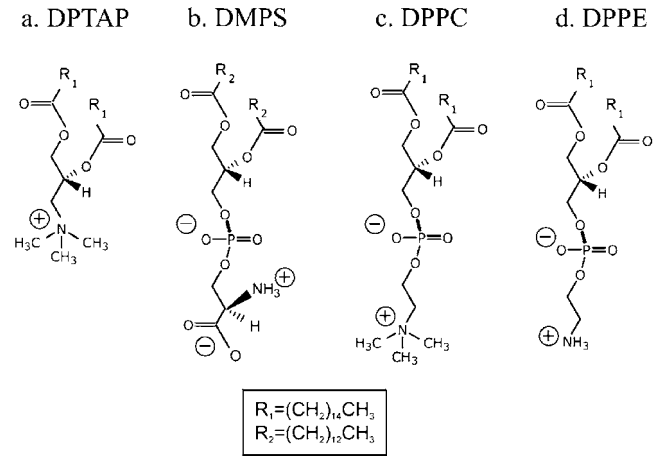

Figure 2. Chemical structures of four different lipids studied in this paper: (a) 1,2-dipalmitoyl-3-trimethylammoniopropane, chloride salt (DPTAP); (b) 1,2-dimyristoyl-*sn*-glycero-3-[phospho-L-serine], sodium salt (DMPS); (c) 1,2-dipalmitoyl-*sn*-glycero-3-phosphocholine (DPPC); and (d) 1,2-dipalmitoyl-*sn*-glycero-3-phosphoethanolamine (DPPE). DPTAP has a net positive charge, DMPS has a net negative charge, and both DPPC and DPPE are zwitterionic.

2. Materials and Methods

Four lipids—1,2-dipalmitoyl-3-trimethylammoniopropane, chloride salt (DPTAP); 1,2-dimyristoyl-*sn*-glycero-3-[phospho-L-serine], sodium salt (DMPS); 1,2-dipalmitoyl-*sn*-glycero-3-phosphocholine (DPPC); and 1,2-dipalmitoyl-*sn*-glycero-3-phosphoethanolamine (DPPE)—were each purchased from Avanti Polar Lipids in powder form and used as received (see Figure 2 for lipid structures). We created monolayers of each lipid by dissolving the lipids in chloroform (DPPC and DPPE) or a 9:1 mixture of chloroform and methanol (DPTAP and DMPS) (2 mg/mL) and then adding this mixture dropwise over an aqueous subphase. All measurements were conducted with monolayers in the lipid condensed phase (at surface pressures between 35 and 40 mN/m). For the static VSF measurements, this aqueous subphase was composed of D_2O purchased from Cambridge Isotope Laboratories, specified by the manufacturer to be 99.96% pure and used as received, while for all IR pump−VSF probe measurements the aqueous subphase was H_2O first distilled and then filtered through a Millipore unit to a final resistivity of 18.2 MΩ·cm. Troughs used in these experiments were home-built, fixed size, and made of either Teflon or Teflon-coated aluminum.

The four lipids under study here are fairly different: DPTAP is a cationic lipid; DMPS is an anionic lipid, present in the inner leaflet of the biological membrane; DPPC or lecithin is a lipid with a zwitterionic phosphocholine headgroup (zero net charge) and is the main constituent of the outer leaflet of eukaryotic cells. Finally, DPPE or cephalin is a lipid with a zwitterionic phosphoethanolamine headgroup and is found in all living cells. DPPC is the N-methylated form of DPPE, and thus a significant difference between the two zwitterionic lipids is expected to be the size of their respective headgroups.

The static VSF setup has been described in detail elsewhere.[59,60] Briefly, we employ a regeneratively amplified Ti:sapphire system

(48) McGuire, J. A.; Shen, Y. R. *Science* **2006**, *313* (5795), 1945–1948.
(49) Smits, M.; Ghosh, A.; Sterrer, M.; Müller, M.; Bonn, M. *Phys. Rev. Lett.* **2007**, *98* (9), 098302.
(50) Smits, M.; Ghosh, A.; Bredenbeck, J.; Yamamoto, S.; Muller, M.; Bonn, M. *New J. Phys.* **2007**, *9*, 390.
(51) Bredenbeck, J.; Ghosh, A.; Smits, M.; Bonn, M. *J. Am. Chem. Soc.* **2008**, *130* (7), 2152–2153.
(52) Ghosh, A.; Smits, M.; Bredenbeck, J.; Bonn, M. *J. Am. Chem. Soc.* **2007**, *129* (31), 9608–9609.
(53) Ghosh, A.; Smits, M.; Bredenbeck, J.; Dijkhuizen, N.; Bonn, M. *Rev. Sci. Instrum.* **2008**, *79* (9), 093907.
(54) Ghosh, A.; Campen, R. K.; Sovago, M.; Bonn, M. *Faraday Discuss.* **2009**, *141*, 145–159.
(55) Eftekhari-Bafrooei, A.; Borguet, E. *J. Am. Chem. Soc.* **2009**, *131* (34), 12034–12035.
(56) Eftekhari-Bafrooei, A.; Borguet, E. *J. Am. Chem. Soc.* **2010**, *132* (11), 3756–3761.
(57) Cowan, M.; Bruner, B.; Huse, N.; Dwyer, J.; Chugh, B.; Nibbering, E.; Elsaesser, T.; Miller, R. *Nature* **2005**, *434* (7030), 199–202.
(58) Kraemer, D.; Cowan, M. L.; Paarmann, A.; Huse, N.; Nibbering, E. T. J.; Elsaesser, T.; Miller, R. J. D. *Proc. Natl. Acad. Sci. U.S.A.* **2008**, *105* (2), 437–442.
(59) Smits, M.; Sovago, M.; Wurpel, G. W. H.; Kim, D.; Mueller, M.; Bonn, M. *J. Phys. Chem. C* **2007**, *111* (25), 8878–8883.
(60) Sovago, M.; Wurpel, G. W. H.; Smits, M.; Muller, M.; Bonn, M. *J. Am. Chem. Soc.* **2007**, *129* (36), 11079–11084.

(Legend; Coherent Inc.) that is optimized for the production of ≈100 fs pulses centered at 800 nm with a bandwidth of 12 nm. A fraction of a pulse (1 mJ/pulse) of this 800 nm light is used to generate tunable mid-IR pulses by use of a commercially available optical parametric amplifier (OPA) and difference frequency generation (DFG) unit (TOPAS; Light Conversion, Vilnius, Lithuania) while another pulse fraction of 0.5 mJ is spectrally narrowed by use of an etalon. After IR generation and 800 nm spectral narrowing, both beams are passed through half-wave plates and polarizers and impinge on the sample in a reflection geometry at angles of 40° and 35° with respect to the surface normal (IR and visible, respectively). After the sample, all remaining 800 nm light is filtered out and the VSF signal is focused into a spectrograph (Acton Instruments) in which it is dispersed, via a grating, and focused onto an electron-multiplied charge-coupled device (emCCD) camera (Newton; Andor Technologies). All spectra reported in this study were collected under the ssp polarization condition (s-polarized SF, s-polarized visible, p-polarized IR). All measurements were conducted at 21.5 °C. To correct for the dependence of the spectral response on the input IR and visible pulses, the measured spectra were divided by the nonresonant spectra taken from z-cut quartz. Our OPA/DFG setup generates substantially more IR in the 2200−2600 cm^{-1} region than the 3100−3600 cm^{-1} region. For this reason we take static spectra over a D_2O subphase, rather than an H_2O subphase. The OD stretch spectra of interfacial D_2O is the same as the OH stretch spectra of interfacial H_2O after mass differences are accounted for. The frequency axis is therefore readily converted to H_2O (see Figure 1).

The IR pump−VSF probe set up has also been described previously.[50,53] Briefly, a Ti:sapphire oscillator (Mira; Coherent Inc.) is used to seed a regenerative/multipass amplifier (Titan; Quantronix). The amplifier output is 800 nm, 100 fs pulses with an energy of 3.5 mJ/pulse and a repetition rate of 1 kHz. One millijoule of this pulse energy is used in a commercial optical parameteric amplification unit (TOPAS; Light Conversion, Vilnius, Lithuania) to produce an idler field centered at a wavelength of 2200 nm. This field is then frequency-doubled in a β barium borate crystal and mixed with 2 mJ of the 800 nm Ti:sapphire output to generate the difference frequency in a $KTiO_4$ (KTP) crystal, leading to the production of 3000 nm pulses of 120 fs length and >80 μJ/pulse energy employed for the IR pump. After generation of the IR pump, the amplified doubled idler and 800 nm pulse were used again in a second KTP crystal to generate the IR portion of the VSF probe. This second IR generation process yielded pulses of ∼120 fs with energies of 8−15 μJ/pulse. The visible portion of the VSF probe was created from the 800 nm light left over from the idler generation. This residual light is spectrally narrowed by use of a home-built pulse shaper to a bandwidth of 10 cm^{-1}. After generation, all three beams are passed through polarizers and $\lambda/2$ plates, after which they are aligned in the same plane (normal to the lipid monolayer) and sent toward the sample with incident angles of 46°, 50°, and 56° relative to the sample surface normal (IR pump, IR probe, and VIS probe respectively). All beams were focused and overlapped at the monolayer and the VSF emission was collected in reflection, frequency-filtered, focused into a spectrograph (Acton Instruments), dispersed on a grating, and the resulting spectra were captured by use of an emCCD camera (Andor Technologies). To correct for possible long-term laser power fluctuations, each IR pump−VSF probe spectra was normalized by an unpumped spectra obtained by chopping the 1 kHz IR pump to 500 Hz and recording a pumped/unpumped ratio every two laser shots. The thus obtained normalized, spectrally integrated VSF spectra were measured as a function of the delay time (Δt) between the IR pump and the VSF probe pair and provide the dynamics traces that reflect the vibrational relaxation of lipid-bound water. The delay time was set by use of a mechanical delay line for the IR pump, and the time transients we present are generated by integrating the entire normalized VSF spectrum at each delay time point. The time-zero and instrument response for the experiments were determined by monitoring the $\chi^{(3)}$ process of infrared−infrared−visible sum-frequency signal as a function of the delay between the pump and probe pulses for the sample under study. For each lipid surface, differential SFG pump−probe transients are recorded at four different center frequencies of the IR pulses, from strongly H-bonded water (3200 cm^{-1}) to weakly H-bonded water (3500 cm^{-1}), in steps of 100 cm^{-1}. The bandwidth of the IR pulses is 150 cm^{-1}. All IR pump−VSF probe transients presented in this report were collected under sspp (SF, vis, IR probe, IR pump) polarization conditions.

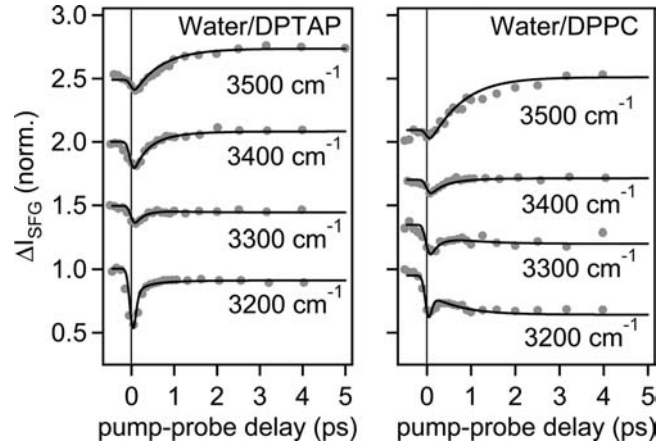

Figure 3. One-color IR pump−VSF probe transients for (left) DPTAP/water and (right) DPPC/water interfaces, recorded at four different IR pump−probe frequencies as a function of delay time. The 3300, 3400, and 3500 cm^{-1} traces are offset for clarity. Black lines are the results of the simulations described in the text.

3. Results

Static VSF spectra covering the frequency window of the OD (OH) stretch of interfacial water beneath DPPE, DPPC, DPTAP, and DMPS monolayers are shown in Figure 1. For each lipid type, the spectral response of the interfacial water has a different amplitude (charged lipids are larger), central frequency, and possibly different line width, as might be expected given the chemical differences between the lipids. However, despite significant differences in interfacial molecular structure (see Figure 2), the spectral response of the interfacial water shows strong similarities: for all lipids the OD (OH) response is well over 100 cm^{-1} wide and shows an apparent double peak. Prior work by some of us has shown that this double-peaked response is not the result of quasi-static structural types of water but rather intramolecular coupling between the fundamental vibration of the water stretch and the overtone of the water bend.[27−29]

The results of IR pump−VSF probe experiments beneath DPTAP and DPPC monolayers are shown in Figure 3 (results for DMPS and DPPE are qualitatively similar to those for DPTAP and DMPS and are shown in the Supporting Information). At all frequencies these transients show an initial decrease (bleach) shortly after $\Delta t = 0$ due to the excitation of the OH stretch mode to its first vibrational state. Following this bleach, all transients at all frequencies show a recovery that is incomplete at lower frequencies (e.g., for DPTAP at 3200 cm^{-1} the signal reaches 0.9 at 5 ps) and exceeds the original signal levels at high frequencies (e.g., for DPTAP at 3500 cm^{-1} the signal reaches 1.2 at 5 ps). These observations of bleaching signals at short delays followed by frequency-dependent signal levels at long times are common to all IR pump−VSF probe studies of interfacial water.[48,49,52,55,56]

The frequency-dependent signal levels at long delay times can be explained by a heating effect. At large time delays, the energy of the pump IR pulse is fully equilibrated over the focus, leading to an increase in temperature of ~10 K. Static VSF spectra of the hydrogen-bonded OH stretch of interfacial water at the lipid/H_2O interface have demonstrated that this resonance blue-shifts and narrows with increasing temperature.[50] Because of this effect of temperature on the OH VSF spectrum, we expect, as is indeed observed, that the 3200 cm^{-1} signal is lower at $\Delta t = 5$ ps than the signal at negative delay and that the 3500 cm^{-1} signal is higher. It should be noted that this heating effect is the result of a single laser shot. We avoid persistent heating effects by employing a 500 Hz (i.e., half the probe frequency) pump pulse and by placing the sample in a rotating trough. These two measures ensure that the heating effect of a single laser pulse has dissipated before the next pulse arrives.

Further inspection of Figure 3 allows for four additional qualitative observations. First, for the charged lipids, the bleach in the IR pump−VSF probe transients is larger than for the uncharged lipids. Inspection of Figure 1 suggests that the amplitude of the OH stretch in the static VSF spectra is also larger for water near charged than uncharged lipids. The observation that VSF spectral amplitude of the OH stretch of interfacial water is larger for water near charged interfaces is general, and this enhancement has been described to be the result of a combination of additional alignment of water molecules near the interface by the interfacial electric field and a bulk-sensitive $\chi^{(3)}$ effect. The observed larger bleach for water near charged lipids is consistent with water molecules near this interface being preferentially aligned with respect to the surface normal and this alignment allowing for more efficient excitation of the water dipoles with the p-polarized pump light employed in this study. Second, we observe that for the neutral lipids the (partial) decay of the bleach is followed by a second loss of signal. Third, for all lipid types, inspection of Figure 4 suggests the recovery of the signal at 3200 cm^{-1} is significantly more rapid than at 3300−3500 cm^{-1}. Finally, for all lipids the maximum bleach appears to occur nearly instantaneously for 3200 cm^{-1} and generally appears to be delayed, relative to $\Delta t = 0$, for all other frequencies. These observations are consistent with a scenario in which vibrational relaxation at 3200 cm^{-1} is faster than that in the 3300−3500 cm^{-1} region. To be more quantitative, it is necessary to model the data.

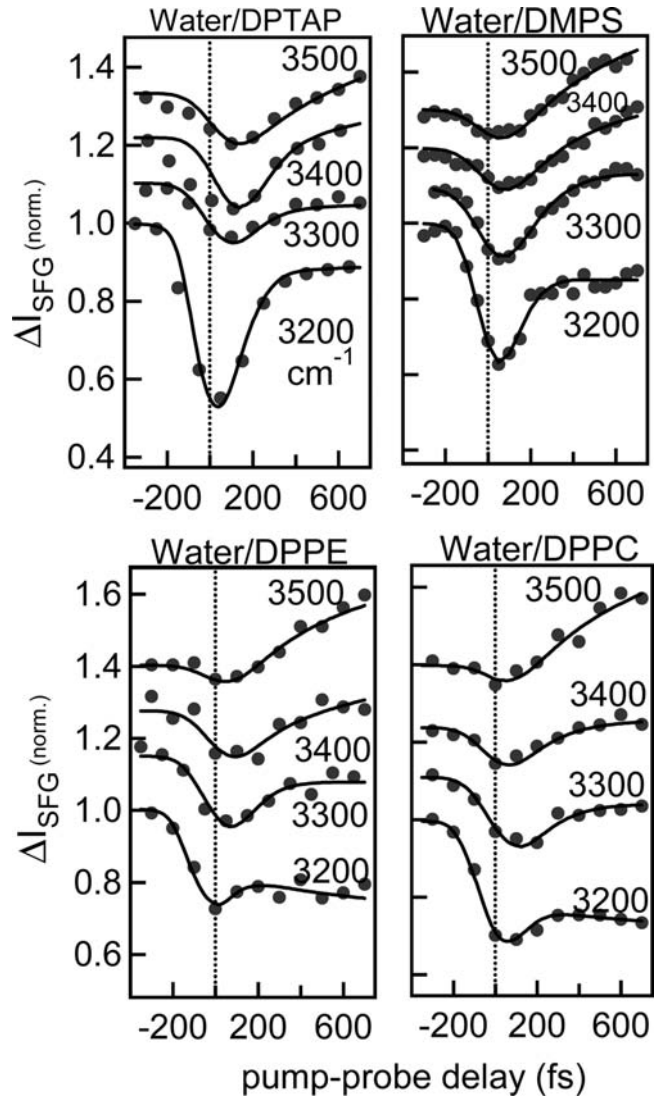

Figure 4. Pump−probe traces zoomed in around zero delay times (vertical dotted lines) for the four different lipids. It is apparent from the data that at 3200 cm^{-1} the bleach recovery is more rapid than at other frequencies (largely complete by 400 fs, whereas at 3300−3500 cm^{-1} the bleach recovery takes more than 600 fs) and that the bleach maximum for the 3300−3500 cm^{-1} traces is delayed relative to that of the 3200 cm^{-1} trace. Both observations indicate that at 3200 cm^{-1} the vibrational lifetime for the response is significantly shorter than at frequencies above 3300 cm^{-1}. The lines are the results of simulations described in the text, which assume homogeneous behavior from 3300 to 3500 cm^{-1}, with an effective T_1 of 180 fs, and fast vibrational relaxation at 3200 cm^{-1} ($T_1 = 50$ fs), without energy exchange for water at that frequency. At all frequencies $\tau_{eq} =$ 600 fs.

4. Analysis and Discussion

The rates and shapes of signal recovery at 3300, 3400, and 3500 cm^{-1} are qualitatively similar to those previously observed at the water/air[49] and water/silica interfaces[48] as well as for water confined in small reverse micelles.[61] For these three systems, it was concluded that the dynamics are homogeneous; that is, that the dynamical response can be described by the same time constants at all frequencies. This homogeneity was attributed to ultrafast (sub-50 fs) energy transfer between OH oscillators located in the bulk and at the interface, with the result that any excitation samples all possible hydrogen-bonding geometries. Over a 5 ps time scale, the resulting dynamics in the systems at different frequencies could thus be described by two frequency-independent time constants: the intramolecular vibrational relaxation time constant (T_1) and a second time constant (τ_{eq}) that characterizes the equilibration process of the excess quanta of excitation energy over all degrees of freedom and involves a reorganization of the hydrogen-bond network.

Given the similarities between the responses measured here and that in the above-mentioned systems, we apply a similar model to the different lipid interfaces. This model (details of which can be found in the Supporting Information) describes the excitation from the ground ($v = 0$) to the first vibrationally excited state ($v = 1$), after which vibrational relaxation occurs with time constant T_1 to a state $v = 0^*$, in which a nonthermal combination of accepting modes is excited. The state $v = 0^*$ then relaxes to $v = 0^{**}$ with time constant τ_{eq}, typically in the

(61) Dokter, A.; Woutersen, S.; Bakker, H. *Phys. Rev. Lett.* **2005**, *94* (17), 178301.

range 0.5−1 ps.[62,63] This simple model results in a set of coupled differential equations that describe the time-dependent populations in the four relevant energy levels of individual OH groups ($\upsilon = 0$; $\upsilon = 1$; $\upsilon = 0^*$; and $\upsilon = 0^{**}$). The relaxation time scales are fixed at 180 and 600 fs—values obtained from previous measurements of vibrational dynamics of bulk water that have successfully fit similar traces at the air/water and silica/water interface at circumneutral pH—and are independent of both frequency and lipid type. The cross sections for generating VSF signal from the different levels are allowed to be frequency-dependent. Such a homogeneous model can describe the data sets for all lipids at 3300, 3400, and 3500 cm^{-1} (shown in Figures 3 and 4 and in the Supporting Information) but cannot account for the faster dynamics observed at 3200 cm^{-1}; a smaller T_1 is required.

A possible explanation for the faster dynamics at 3200 cm^{-1} is that relaxation at this OH frequency is too fast to allow excitation transfer to OH oscillators at higher frequencies. To test this hypothesis, we modeled the concurrent processes of vibrational relaxation and spectral equilibration due to energy transfer by dividing the static SFG spectrum into 240 discrete bins of 2 cm^{-1} width. The excitation pulse determined the spectral profile of the initial pump-induced bleach. At each simulation time step of 2 fs, part of the bleach of each bin is allowed to hop to the other bins, and each bin thus decays due to energy transfer with a time-dependent rate (k_f) taken to be equal to the Förster rate of bulk water and given by[35]

$$k_f(t) = \frac{(4/3)\pi^{3/2}[\mathrm{OH}]N_a(r_0^3/\sqrt{T_1})}{2\sqrt{t}} \qquad (1)$$

In this expression, [OH] is the bulk concentration of OH oscillators of 111 M (2 × 55.5 M), N_a is Avogadro's number, r_0 is the Förster radius in decimeters (2.1×10^{-9} dm) and T_1 is the average vibrational lifetime across the band, taken to be 180 fs. It should be noted that the Förster radius is defined as the distance between two OH oscillators for which there is 50% probability that the excitation is transferred within the lifetime T_1. Hence, choosing a different value of T_1 would lead to a corresponding change of r_0 that keeps the coupling term, $r_0^3/T_1^{0.5}$, that characterizes the dipole−dipole interaction between OH oscillators in water, constant. Note that within this model the population that leaves the bins with the above equation is redistributed over the entire spectral distribution following the probability distribution of the spectral profile. Hence, if a spectral hole would be burnt, the Förster transfer will lead to an evolution to the equilibrium spectral shape.

In parallel with Förster transfer, the bleach intensity decays due to vibrational relaxation, with a rate that depends on frequency. This frequency dependence can be described in several different ways. One approach would be to describe the frequency dependence from the overlap of the OH stretch vibration with the overtone of the bend vibration.[63] This overlap will depend on the central frequency and line width of the homogeneous band hidden under the OH stretch response. Unfortunately, these parameters are not known. Therefore we chose a different approach. Previous studies[64−66] have shown that the frequency dependence of the vibrational lifetime of the

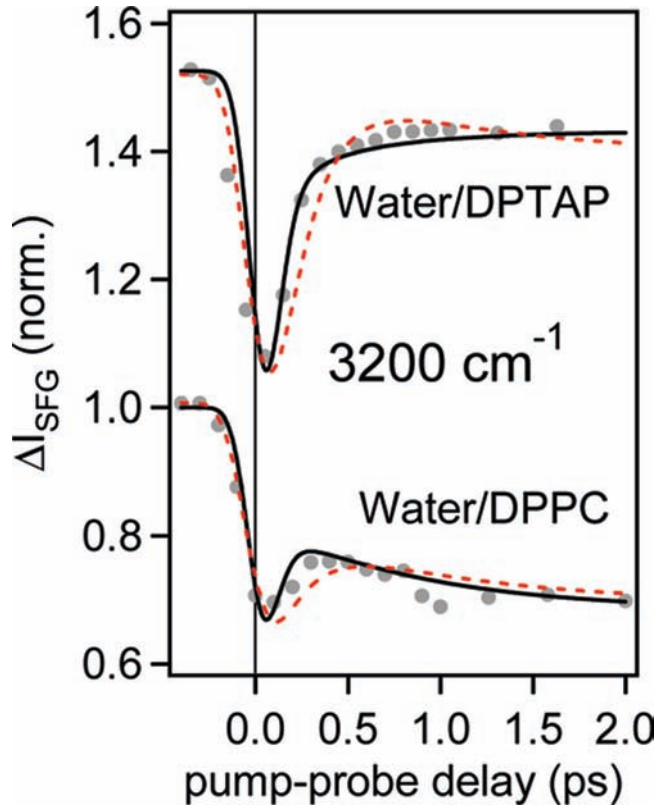

Figure 5. One-color IR pump−VSF probe transients at 3200 cm^{-1} for DPPC/water and DPTAP/water interfaces. In both cases, the solid black line is the result of simulations described in the text with $T_1 = 50$ fs, and the dashed line shows the homogeneous model with $T_1 = 180$ fs. Clearly the homogeneous model, which works well for the 3300−3500 cm^{-1} traces, breaks down at 3200 cm^{-1}.

OH vibration of hydrogen-bonded systems can be phenomenologically described with the expression:

$$T_1\ (\text{in ps}) = \frac{22500}{(3700 - \nu)^2} \qquad (2)$$

This expression yields $T_1 = 180$ fs at 3350 cm^{-1}, where on average most spectral intensity is present, in agreement with bulk reports of T_1.[35,57] Combining the description of excitation transfer and vibrational relaxation results in a system of 240 coupled differential equations describing the complete dynamics of all bins, which we solved using a fourth-order Runge−Kutta algorithm.

In our four-level model, the population decay of the OH groups results in the population of an intermediate state that in turn relaxes to a thermal state with a time constant τ_{eq}. In calculating the transients, we ascribed a frequency-dependent amplitude to the thermal state, in agreement with the change in the static SFG spectrum upon an increase in temperatures. Setting the value of τ_{eq} to its bulk value of 600 fs[62,63] for experiments at all four frequencies produces good agreement with data.

Using the above approach, and $\tau_{eq} = 600$ fs, we find the relaxation rate of the calculated transients at 3200 cm^{-1} to be practically the same as that at higher frequencies and slower than the data (see Figure 5). Evidently, assuming energy transfer

(62) Lock, A. J.; Woutersen, S.; Bakker, H. J. *J. Phys. Chem. A* **2001**, *105* (8), 1238–1243.
(63) Lock, A.; Bakker, H. *J. Chem. Phys.* **2002**, *117* (4), 1708–1713.
(64) Miller, R. E. *Science* **1988**, *240* (4851), 447–453.
(65) Staib, A.; Hynes, J. T. *Chem. Phys. Lett.* **1993**, *204* (1−2), 197–205.
(66) Woutersen, S.; Emmerichs, U.; Nienhuys, H. K.; Bakker, H. J. *Phys. Rev. Lett.* **1998**, *81* (5), 1106–1109.

between all water molecules in the band, that is, equilibration over the full SFG spectrum, yields a clearly too slow relaxation at 3200 cm^{-1}. At this point it should be noted that this result is quite robust to the choice of the description of the frequency dependence of the vibrational lifetime T_1. For instance, describing this frequency dependence from the overlap of the (homogeneous) OH stretch band and the overtone of the bending mode with an estimated homogeneous width of 140 cm^{-1} [67] leads to a weaker frequency dependence of T_1 than provided by eq 1. Hence, such a description also gives a too-long T_1 of ~180 fs at 3200 cm^{-1}. We thus conclude that the OH oscillators at 3200 cm^{-1} are not coupled in the same manner to the other OH oscillators as is the case in bulk liquid water. Instead, the OH oscillators at 3200 cm^{-1} appear to be decoupled from the other OH oscillators, at least on a subpicosecond time scale.

We refined the model to include two specific water subensembles corresponding to two spectral components above and below 3250 cm^{-1}. The two spectral domains were separated by use of a sigmoidal function of width 25 cm^{-1} (note that the results are insensitive to the precise value). The resulting spectral subsets are shown as gray lines in the spectra shown in Figure 1. We note that while this spectral decomposition subdivides the water into strongly and weakly hydrogen-bonded subensembles, we do not correlate this specifically to "icelike" and "liquidlike" structures. Rather, we expect a continuous distribution of hydrogen-bond strengths, with reduced spectral diffusion in the lower tail of this distribution. The spectral equilibration and vibrational relaxation of the high-frequency part of the spectrum was modeled as described above. The response of the low-frequency component is assumed to be homogeneous, showing a T_1 of 50 fs at all frequencies and no Förster transfer to the high-frequency band.

The results of the two-component analysis are shown in Figures 4 and 5. It is apparent that this simple model describes the data very well, providing support for the notion that two distinct subensembles of water exist for these water/lipid interfaces. For relatively weakly hydrogen-bonded water (3300−3500 cm^{-1}), intermolecular vibrational energy transfer dominates the response, and the different water molecules are spectrally indistinguishable, an effect presumably caused by the fast energy transfer with the bulk also observed for water at the water−air interface (although we note that, strictly speaking, the data reported here could also be accounted for by in-plane energy transfer that is quantitatively bulklike). It is interesting to note that the spectrum of the subensemble at 3300−3500 cm^{-1} constituting the blue part of the spectrum (see Figure 1) closely resembles the vibrational spectrum of bulk water. In summary, for the water molecules at 3200 cm^{-1}, the T_1 apparently is extremely fast, $\approx$ 50 fs, and the OH oscillators are decoupled from those in bulk. While $T_1 = 50$ fs offers the best description of the 3200 cm^{-1} data, given the signal-to-noise ratio in our experiment, we conservatively conclude that $T_1 < 80$ fs at 3200 cm^{-1}.

The results thus indicate that two types of water molecules exist for all the different water/lipid interfaces: water that behaves, in terms of both its vibrational frequency and vibrational dynamics, bulklike (3300−3500 cm^{-1}; $T_1 = 180 \pm 35$ fs) and water that is very strongly H-bonded (3200 cm^{-1}) and exhibits faster vibrational relaxation ($T_1 < 80$ fs) and suppressed energy transfer. Such strongly coupled hydrogen bonds between the interfacial water and the lipid headgroups may be attributed to water interacting with strong H-bond acceptor groups like the phosphate moieties present on the headgroups. Absent the phosphate group, there is no strong acceptor that appears on the lipids. Given the absence of phosphate groups for DPTAP (where this strongly bound water is also observed), an alternative explanation may be water that is near but not hydrogen-bonded to the carbonyls (thus accounting for the low local density) and is a double (or triple) acceptor, single donor to another water molecule.[68] Water arranged in this manner may exhibit the three properties observed experimentally here: stronger H-bonding, faster relaxation due to the increased anharmonicity induced by that same strong hydrogen bond, and a reduced water−water energy transfer rate owing to the locally reduced water density (because of the space taken up by the lipid headgroup[69,70]).

Thus, for a subpopulation of the interfacial water, interaction with the lipid headgroup decouples these water molecules from the underlying bulk, structurally and energetically. Apparently, intermolecular water−lipid forces are strong enough to lead to the formation of strongly bound water, which presumably exchanges with the bulk on time scales that are long compared to the typical measurement time in our experiments. This conclusion is consistent with NMR studies of partially hydrated bilayers, which have shown that the time scale on which exchange occurs between bulk water and water associated with lipid headgroups is on the order of ~100 ps.[8] It is remarkable that the observed water dynamics are independent of the details of the specific lipid. Despite the differences between the headgroups of the different lipids, which one would expect to give rise to differences in hydrogen-bonding properties, the frequency-dependent vibrational dynamics are very similar for all these lipids, with strongly hydrogen-bonded water exhibiting fast, ~80 fs decay. Apparently, the similarities in the way the different lipids bind water are larger than their differences with respect to the vibrational dynamics of water.

Prior work suggests that strongly hydrogen-bonded, structurally isolated, membrane-bound water, such as we have observed, may be important for a variety of biological processes. For instance, for proton transfer at the cell membrane, such strongly hydrogen-bonded water may be involved in the fast in-plane transfer of protons: for highly ordered water structures, it has been proposed that proton transfer is enhanced.[71,72] This structural type of water is also thought to be necessary for the function of membrane-bound, voltage-sensing proteins and important for the function of transmembrane proteins more generally.[1−3,73,74] In the absence of proteins, the interaction of this subensemble of water molecules with the lipid headgroups is thought to be important for the quantitative determination of membrane dipole potentials and for understanding the possibility of

(67) Gale, G. M.; Gallot, G.; Hache, F.; Lascoux, N.; Bratos, S.; Leicknam, J. C. *Phys. Rev. Lett.* **1999**, *82* (5), 1068–1071.
(68) Lenz, A.; Ojamae, L. *J. Phys. Chem. A* **2006**, *110* (50), 13388–13393.
(69) Marrink, S. J.; Berkowitz, M.; Berendsen, H. J. C. *Langmuir* **1993**, *9* (11), 3122–3131.
(70) Dominguez, H.; Smondyrev, A. M.; Berkowitz, M. L. *J. Phys. Chem. B* **1999**, *103* (44), 9582–9588.
(71) Mann, D. J.; Halls, M. D. *Phys. Rev. Lett.* **2003**, *90*, 195503.
(72) Dellago, C.; Naor, M. M.; Hummer, G. *Phys. Rev. Lett.* **2003**, *90*, 105902.
(73) Zaccai, G. *Biophys. Chem.* **2000**, *86* (2−3), 249–257.
(74) Disalvo, E. A.; Lairion, F.; Martini, F.; Tymczyszyn, E.; Frias, M.; Almaleck, H.; Gordillo, G. J. *Biochim. Biophys. Acta:, Biomembr.* **2008**, *1778* (12), 2655–2670.

membrane penetration by a variety of small molecules.[74,75] Put generally, then, the results of this study suggest we now have the capacity to directly probe water bound near the base of lipid headgroups. We expect therefore that in future experiments with more complicated model systems we will be able to gain a detailed, molecular-level picture of the role of this water in a variety of biophysical processes in membranes. Such insight is unique to the type of IR pump−VSF probe experiments we have described and should be of general utility to those interested in these important and fascinating problems.

5. Summary and Conclusions

Four different model biological lipid/water interfaces were studied, namely, monolayers of DPTAP, DMPS, DPPC, and DPPE on water, and time-resolved SFG was used to elucidate the vibrational dynamics of the water molecules interfacing the lipid monolayers. We find two predominant mechanisms of vibrational relaxation, irrespective of the details of the lipid monolayer system studied. For medium-strength to weakly hydrogen-bonded water molecules (3300−3500 cm^{-1}), a Förster-type energy transfer among neighboring water molecules dominates the energy dissipation mechanism, which randomizes the excitation on very short time scales, and subsequent relaxation occurs essentially with a time constant of ∼180 fs, a phenomenon previously also observed in bulk and neat water/air interfaces. For strongly hydrogen-bonded water molecules (3200 cm^{-1} OH stretch fundamental), vibrational relaxation occurs on time scales appreciably shorter than the pulse duration, presumably through the hydrogen-bond modes associated with the lipid headgroup moieties. These water molecules do not show rapid intermolecular energy exchange with other interfacial or bulk water molecules, probably as a result of the reduced local water density in the lipid headgroup region.

Acknowledgment. This work is part of the research program of the Stichting Fundamenteel Onderzoek der Materie (Foundation for Fundamental Research on Matter) with financial support from the Nederlandse Organisatie voor Wetenschappelijk Onderzoek (Netherlands Organization for the Advancement of Research). Financial support was also provided from the JSPS Postdoctoral Fellowships for Research Abroad (to S.Y.) and the Marie Curie Incoming International Fellowship (to R.K.C). We are grateful to Ellen Backus for her expert help and fruitful discussions.

Supporting Information Available: A figure showing IR pump−VSF probe data for interfacial water at DPPE and DMPS lipid monolayers, as well as a detailed description (text, equations, and three figures) of the four-level model used to fit the data and comparison of this model to that employed in the work of McGuire and Shen[48] and Eftekhari-Bafrooei and Borguet[55] to analyze similar systems. This material is available free of charge via the Internet at http://pubs.acs.org.

JA106194U

(75) Bouchet, A. M.; Frías, M. A.; Lairion, F.; Martini, F.; Almaleck, H.; Gordillo, G.; Disalvo, E. A. *Biochim. Biophys. Acta: Biomembr.* **2009**, *1788* (5), 918–925.